THE ASTROPHYSICAL JOURNAL, 452:L95–L98, 1995 October 20

REVEALING THE EFFECTS OF ORIENTATION IN COMPOSITE QUASAR SPECTRA

JOANNE C. BAKER[1,2] AND RICHARD W. HUNSTEAD[2]
Received 1995 May 16; accepted 1995 August 15

ABSTRACT

We present low-resolution, composite optical spectra for 60 quasars drawn from the 408 MHz–selected Molonglo Quasar Sample. Individual spectra have been co-added according to the ratio of radio core-to-lobe flux density R in order to show global changes as a function of quasar orientation. Compact steep-spectrum (CSS) quasars have been combined separately. With increasing implied viewing angle to the radio-jet axis, we find that (1) the optical continuum steepens, (2) the 3000 Å broad emission feature decreases in relative strength, and (3) the narrow-line equivalent widths, broad-line widths, and Balmer decrements increase. The composites show that reddening is considerable in most lobe-dominated quasars ($A_V \sim 2$–4). Moreover, the extinction appears to be aspect-dependent, which suggests an intrinsic origin for the dust. The CSS composite spectrum is particularly striking, showing evidence for significant reddening, a steep power-law continuum, relatively strong low-ionization narrow-line emission, and no discernible 3000 Å bump.

Subject headings: galaxies: active — quasars: emission lines — quasars: general

1. INTRODUCTION

Orientation has been singled out as a major contributor to the diversity of active galactic nuclei (AGNs), with the assumption that highly anisotropic components dominate the emission in many wave bands. This idea forms the basis of the unified schemes for AGNs (see review by Antonucci 1993). A particularly successful application of this concept has been to draw together the family of radio-loud quasars by the proposition that core- and lobe-dominated quasars are intrinsically similar, differing only in radio-jet axis orientation. Such a picture has prompted the use of the ratio of radio core-to-lobe flux density R as an indicator of jet orientation (e.g., Orr & Browne 1982).

At optical wavelengths, there is mounting evidence that the continuum emission from quasars is also anisotropic. Comparison of the optical magnitudes of samples of core- and lobe-dominated quasars matched in extended flux density (see e.g., Browne & Wright 1985) and the statistical decrease of narrow [O III] λ5007 equivalent widths with increasing R (see, e.g., Jackson & Browne 1991) suggest that the optical continuum is enhanced by some 2–3 mag in core-dominated quasars. Orientation dependence has also been claimed for many broad-line properties (e.g., Jackson & Browne 1991). However, it is generally assumed that the narrow-line emission—arising further (>1 kpc) from the nucleus—is isotropic.

Despite the success of the orientation-based unified models for quasars, they are unable to accommodate all classes, notably compact steep-spectrum (CSS) quasars as well as the radio-quiet majority. CSS sources, comprising ~20% of radio-selected quasars, are intrinsically small (>15 kpc), with most showing complex VLBI radio structures and no obvious flat-spectrum core (see review by Fanti & Fanti 1994). It has been postulated that the unusual radio properties of these sources may be a consequence either of youth or confinement by a dense interstellar medium (ISM).

In this *Letter*, low-resolution, composite quasar spectra, spanning ultraviolet to optical rest-frame wavelengths, are presented as a function of the relative core strength R. Thus, spectral trends are summarized with changing viewing angle. A composite spectrum has also been created for CSS quasars, which differs markedly from the other spectra. Individual quasar spectra have been drawn from the Molonglo Quasar Sample, described briefly below.

2. THE MOLONGLO QUASAR SAMPLE

In order to minimize orientation-dependent selection biases, the Molonglo Quasar Sample (MQS) was selected initially at 408 MHz, where steep-spectrum, extended emission dominates. Sources with $S_{408} > 0.95$ Jy were drawn from the Molonglo Reference Catalogue (Large et al. 1981) in a 10° declination strip ($-20° > \delta > -30°$ and $|b| > 20°$). Optical identifications, estimated to be more than 90% complete (Baker 1994), have been obtained down to a limiting blue magnitude $b_J \sim 22.5$ on the UK Schmidt IIIaJ survey plates and also from R-band CCD images. To date, redshifts are available for 92 of the 101 MQS quasars, spanning the range $z = 0.1$–2.9 (median $z \sim 1$). The sample includes one broad-line radio galaxy plus three BL Lac objects (without redshifts). We assume that the exclusion of the six unconfirmed quasar candidates (3 CSS and 3 lobe-dominated sources) does not introduce significant biases.

Low-resolution (FWHM 25 Å) optical spectra, covering 3400–10000 Å, have been obtained for 72 MQS quasars with the RGO spectrograph and Faint Object Red Spectrograph on the Anglo-Australian Telescope (AAT). Observations were made with the slit at parallactic angle to ensure accurate relative spectrophotometry. Radio core-to-lobe flux density ratios R have been measured from 5 GHz VLA maps at ~1″ resolution. The R-values were K-corrected to an emitted frequency of 10 GHz by use of spectral indices calculated between 408 MHz and 5 GHz. Individual radio maps and optical spectra for the MQS will be published elsewhere.

3. BUILDING THE MQS COMPOSITES

Composite spectra have been assembled from 60 individual AAT spectra for MQS quasars in four subsets: $R \geq 1$,

[1] MRAO, Cavendish Laboratory, Madingley Road, Cambridge CB3 0HE, UK; j.c.baker@mrao.cam.ac.uk.
[2] Department of Astrophysics, School of Physics, University of Sydney, NSW 2006, Australia.

TABLE 1

SPECTRAL MEASUREMENTS FOR MQS COMPOSITES

LINE	$R \geq 1$			$0.1 \leq R < 1$			$R < 0.1$			CSS		
	F_{rel}[a]	W_λ[b] (Å)	Δv[c] (km s^{-1})	F_{rel}	W_λ (Å)	Δv (km s^{-1})	F_{rel}	W_λ (Å)	Δv (km s^{-1})	F_{rel}	W_λ (Å)	Δv (km s^{-1})
Hα	5.0	430	2900	6.1	660	3900	8.2	740	3200	10	520	2300
[O III]	0.8	71	...	0.7	91	...	1.4	250	...	4.1	340	...
Hβ	1.0	90	3500	1.0	135	5400	1.0	170	5800	1.0	83	2500
[O II]	0.1	8	...	0.03	4	...	0.07	16	...	1.0	120	...
Mg II	0.4	43	4100	0.4	75	10200	0.2	71	11200	0.2	36	7000
C III]	0.2	34	6000	0.1	25	5500	0.04	16	6400	0.1	20	9000
C IV	0.3	29	5600	0.4	113	8900	0.2	120	8000	0.2	75	5800
Lyα	0.4	24	5900	...	...	...	...	...	...	0.2	79	7400
Statistical Quantities												
α_{opt}[d]	0.5			0.7			1.0			1.4		
N_Q[e]	13			18			16			13		

[a] Ratio of integrated line flux relative to Hβ.
[b] Rest-frame equivalent width.
[c] Velocity FWHM.
[d] Best-fit power-law spectral index, 1500–6800 Å ($f_\nu \propto \nu^{-\alpha}$).
[e] Number of quasars included in each composite.

$1 > R \geq 0.1$, $R < 0.1$, and CSS. Each composite comprises 13–18 spectra (Table 1). Twelve quasars with either abnormally strong absorption features (intrinsic or atmospheric) or no R-values were excluded.

Systemic redshifts were measured from the prominent narrow lines, where possible [O III] λ5007, to minimize the effects of intrinsic velocity differences between high- and low-excitation lines and to keep the [O III] doublet well resolved. However, for redshifts $z \gtrsim 1$, the mean redshift, including the broad lines, was used. Before combining, the spectra were each shifted to the quasar rest frame, normalized at 3000 Å, and noisy edges trimmed.

For each subset, the spectra were first ordered in redshift, then consecutive pairs of spectra were merged (using the Starlink DIPSO function MERGE), then these pairs were merged, and so on until a final composite was created. In general, weighting was avoided except in cases of particularly noisy or restricted-wavelength spectra, which were reduced in weight by factors of 2–4. The resultant composite spectra are displayed in Figure 1, shown on a log-log scale to emphasize the differences.

By normalizing the spectra at one point, rather than dividing by a fitted continuum, spectral slope characteristics have largely been preserved. However, the spectral shapes may be less reliable near the edge regions (below 1600 Å and above 5000 Å), which come only from the extreme redshifts. The numbers of spectra that contribute to each composite as a function of wavelength are shown in Figure 2.

Line and continuum measurements for each composite spectrum are listed in Table 1 as a guide to global properties. Measurement errors are typically 10%–20% in W_λ, arising mostly from uncertainties in local continuum placement (particularly in the 2000–4000 Å region—the "3000 Å bump"), and somewhat larger, typically 30%, in line ratios and widths. Broad-line blends such as Lyα and N V have not been deconvolved because of the low spectral resolution.

4. COMPARISON OF COMPOSITE SPECTRA

The MQS composite spectra (Fig. 1) reveal clear differences between quasars of different R and between CSS and other quasars. For comparison, the optically selected Large Bright Quasar Survey (LBQS) composite of Francis et al. (1992) is also shown in Figure 1. The main trends are described below (see also Table 1).

4.1. *Trends with R*

Perhaps the most striking trend in Figure 1 is the obvious steepening of the continuum in quasars of decreasing R (see also Table 1). Relative to the continuum, the 3000 Å bump also appears markedly stronger in core-dominated quasars. In addition, at low R, the Hα/Hβ line ratio is considerably larger, and the Balmer lines are weaker relative to the narrow lines. Both the changes in continuum slope and Balmer decrement point to increased reddening in lobe-dominated quasars ($\langle A_V \rangle \sim 2$ for $R < 1$).

In addition, the equivalent widths of the narrow lines, particularly [O III] λ5007 and [O II] λ3727, increase toward low R. For [O III], this has been interpreted as evidence for enhanced optical continuum emission in core-dominated quasars (e.g., Jackson & Browne 1991). A quantitatively similar anticorrelation of [O II] equivalent width with R is present in the MQS. Moreover, this effect appears to be stronger statistically in [O II] (Baker et al. 1994), although it is less clear in Figure 1. A full investigation of anisotropic continuum emission in the MQS will be presented in a later paper.

From high to low R, the broad Balmer line and Mg II λ2798 profiles widen systematically, although the change is most noticeable in comparison of the $R \geq 1$ and $R < 1$ regions. Such a dependence for the broad Hβ line (Wills & Browne 1986) has been taken as strong evidence that Hβ is emitted by gas in a disklike configuration. The trend in Hα FWHM is weaker (Table 1), although this line is known to be blended. A detailed examination of broad-line properties in the MQS is also deferred to a later paper.

4.2. *CSS Quasars*

The most dramatic feature of the CSS composite is the steep, power-law continuum, which is presumably nonthermal in origin. It is possible that the steep slope is due to reddening, and this is supported by the relatively large Balmer decrement ($\langle A_V \rangle \sim 4$). However, no spectral curvature or 2200 Å dust-

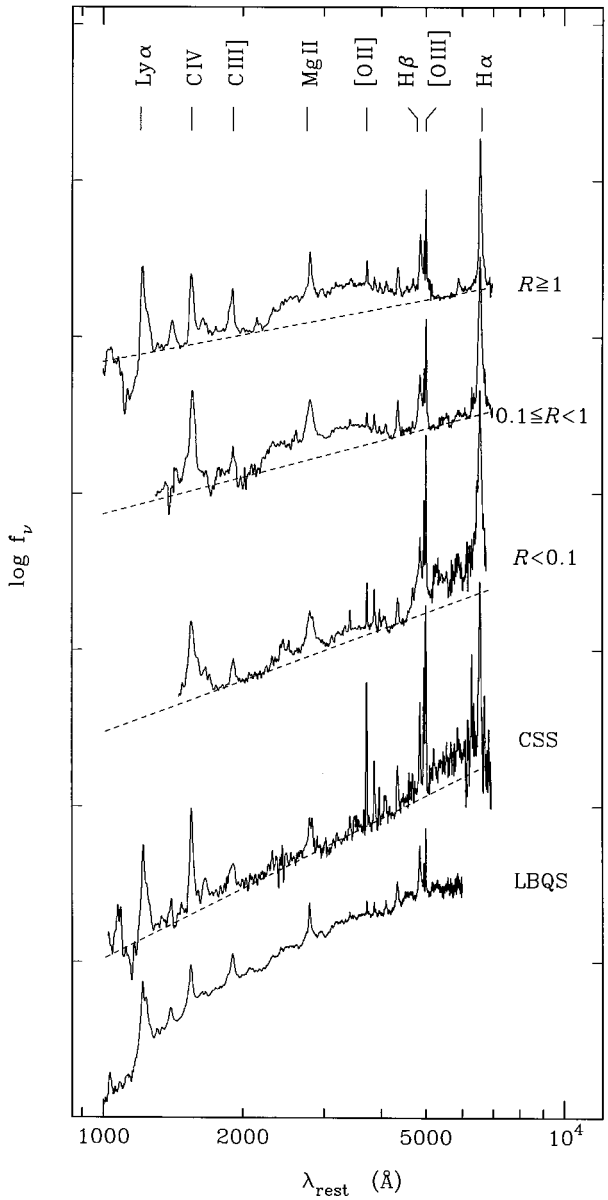

FIG. 1.—Composite spectra for the MQS, separated according to their radio core dominance (see text). Power-law spectral slopes are shown as dashed lines (see Table 1). Also shown is the LBQS composite from Francis et al. (1992). Decades are marked on the vertical axis.

absorption feature (albeit rare in quasar spectra) is observed in the CSS spectrum, which precludes exceptionally large amounts of dust extinction. Alternatively, the continuum may be intrinsically steep. The 3000 Å bump appears to be completely absent in the CSS composite, which perhaps indicates that the ionizing continuum is different from that in other radio-loud quasars. Alternatively, a combination of iron self-absorption and Balmer line reddening may reduce the strength of the feature.

The broad Balmer line wings appear to be comparatively weak in the CSS subsample, perhaps as a consequence of partial obscuration of the broad-line region or simply lower average velocities for the line-emitting gas. Also, the unusually low Lyα/C IV ratio suggests that Lyα photons are heavily absorbed. Self-absorption in broad Mg II λ2798 is preserved in the composite, which points to associated absorption being relatively common in CSS quasars.

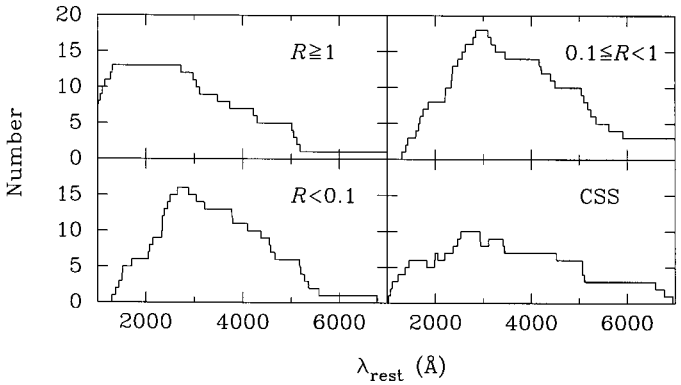

FIG. 2.—Number of spectra contributing to each MQS composite as a function of wavelength. Note the redshift bias in the $R \geq 1$ subsample, which suggests orientation-dependent selection effects in the optical.

The CSS composite also shows exceptionally strong forbidden lines relative to the continuum, especially the low-ionization species. This must imply that either the continuum itself is weak or the narrow-line emission is enhanced.

4.3. *Optically Selected Quasars*

The LBQS composite differs from the MQS most markedly in that the underlying continuum does not follow a simple power law, instead exhibiting a pronounced downturn in the blue. As discussed by Francis et al. (1992), such a falloff may arise through atmospheric dispersion, biases within the composite-building procedure, or evolutionary effects. On the other hand, the curved spectrum may mark an intrinsic difference between radio-quiet and radio-loud quasars.

On the whole, the average line properties of the optically selected LBQS appear to resemble most closely those of core-dominated quasars in Figure 1, which may indicate a preferred viewing direction for optically selected quasars. The most notable differences include the equivalent width of [O III] and the strength of the 3000 Å bump; both are weaker in the LBQS. It should also be noted that the LBQS contains quasars of higher average optical luminosity than the MQS, so ambiguity exists over whether these differences are attributable to radio quietness or optical luminosity.

5. DISCUSSION

Although reddened quasars have been noted before in low-frequency–selected samples (Smith & Spinrad 1980; Mathur 1994), the excess reddening observed in *lobe-dominated* MQS quasars suggests furthermore that the extinction is *orientation dependent*. In accordance with the unified schemes, this implies that larger column densities of dust obscure quasars viewed at larger inclinations to the radio-jet axis. A toroidal dust distribution could account for this trend. In contrast to the simple *opaque* torus, which has been invoked to conceal the central broad-line regions in narrow-line AGNs (Krolik & Begelman 1986), Figure 1 indicates that significant column densities of dust must lie along sight lines *within* the opening angle of the putative torus. In fact, there may not be a well-defined opening angle at all.

As described above, aspect-dependent reddening is also consistent with the proposed unification by orientation of powerful radio galaxies and quasars. An important conse-

quence is that red, lobe-dominated quasars are more likely to be missed on blue survey plates, thus introducing an additional color bias into most quasar samples. Furthermore, heavily reddened, lobe-dominated quasars at moderate redshifts may be misclassified as radio galaxies, which would affect the relative numbers of broad- and narrow-line AGNs.

CSS quasars, though, do not fit neatly into this scheme. Dust reddening, as inferred from the steep continuum and large Balmer decrement, may be significant in these sources. Additionally, thermal optical components, such as the Big Blue Bump, may be absorbed or suppressed. The large equivalent widths of the low-ionization narrow lines, especially [O II] λ3727 and [O I] λ6300, point to the presence of strong interactions between the radio jet and ISM, perhaps mediated by shocks. The presence of a dense ISM is also supported by the self-absorption seen frequently in Mg II, and also in Lyα and C IV. Interestingly, there is evidence to suggest that the CSS and the related gigahertz-peaked spectrum sources may suffer unusually heavy absorption at X-ray energies (Elvis et al. 1994; Baker, Hunstead, & Brinkmann 1995), which suggests a link, perhaps environmental, between the optical and X-ray absorbers.

6. CONCLUSIONS

The composite spectra presented in Figure 1 neatly summarize numerous spectral trends with radio core dominance *R*. Furthermore, the MQS composites present new evidence that the optical continuum slope and Balmer decrements increase in lobe-dominated quasars, suggestive of aspect-dependent reddening. Moreover, the 3000 Å bump weakens markedly at low *R*. The inferred dust geometry can be tied to torus models for radio-loud AGNs but must imply that the torus does not have a sharp opening angle. Comparison with the optically selected LBQS composite of Francis et al. (1992) also reveals clear differences and some similarities between radio-loud and radio-quiet quasars.

The average spectral properties of CSS quasars have been displayed here for the first time and provide a new insight into these enigmatic sources. Enhanced narrow-line emission is evident, along with a steep, nonthermal continuum. The spectral characteristics are consistent with the presence of an unusually dense ISM and may also indicate differences in the shape of the ionizing continuum in CSS quasars. The shock-excitation and absorption signatures in these sources need to be investigated further.

We thank our collaborators Vijay Kapahi and C. R. Subrahmanya, for supplying the radio data for the MQS, and the referee, for valuable comments. J. C. B. is grateful for an RCfTA scholarship at the University of Sydney. R. W. H. acknowledges funding from the Australian Research Council. The LBQS spectrum was used with the kind permission of Paul Francis.

REFERENCES

Antonucci, R. R. J. 1993, ARA&A, 31, 473
Baker, J. C. 1994, Ph.D. thesis, Univ. of Sydney
Baker, J. C., Hunstead, R. W., & Brinkmann, W. 1995, MNRAS, in press
Baker, J. C., Hunstead, R. W., Kapahi, V. K., & Subrahmanya, C. R. 1994, in ASP Conf. Proc. 54, The Physics of AGN, ed. G. V. Bicknell, M. A. Dopita, & P. J. Quinn (San Francisco: ASP), 195
Browne, I. W. A., & Wright, A. E. 1985, MNRAS, 213, 97
Elvis, M., Fiore, F., Wilkes, B., McDowell, J., & Bechtold, J. 1994, ApJ, 422, 60
Fanti, C., & Fanti, R., 1994, in ASP Conf. Proc. 54, The Physics of AGN, ed. G. V. Bicknell, M. A. Dopita, & P. J. Quinn (San Francisco: ASP), 341
Francis, P. J., Hewett, P. C., Foltz, C. B., & Chaffee, F. H. 1992, ApJ, 398, 476
Jackson, N., & Browne, I. W. A. 1991, MNRAS, 250, 422
Krolik, J. H., & Begelman, M. C. 1986, ApJ, 308, L55
Large, M. I., Mills, B. Y., Little, A. G., Crawford, D. F., & Sutton, J. M. 1981, MNRAS, 194, 693
Mathur, S. 1994, ApJ, 431, L75
Orr, M., & Browne, I. W. A. 1982, MNRAS, 200, 1067
Smith, H. E., & Spinrad, H. 1980, ApJ, 236, 419
Wills, B. J., & Browne, I. W. A. 1986, ApJ, 302, 56

THE ASTROPHYSICAL JOURNAL, 461:L59, 1996 April 10

ERRATA

In the Letter "Revealing the Effects of Orientation in Composite Quasar Spectra" by Joanne C. Baker and Richard W. Hunstead (ApJ, 452, L95 [1995]), a correction should be made on page L95. In accordance with the definition of compact, steep-spectrum sources in the third paragraph of the Introduction, the second sentence should state the condition "< 15 kpc" rather than "> 15 kpc."

In the Letter "Facts and Artifacts in Interstellar Diamond Spectra" by H. Mutschke, J. Dorschner, Th. Henning, C. Jäger, and U. Ott (ApJ, 454, L157 [1995]), there exists a series of misprints: in all chemical formulae, single bonds have been replaced by double bonds. The only case in which the double bonds are correct is C═O.

In the Letter "Interferometric Imaging of the Sunyaev-Zeldovich Effect at 30 GHz" by John E. Carlstrom, Marshall Joy, and Laura Grego (ApJ, 456, L75 [1996]), the printer included the wrong figures (Plates L10–L14). The correct Figures 1–4 with captions are reproduced here as Plates L11–L14.

THE ASTROPHYSICAL JOURNAL, 468:L131, 1996 September 10

ERRATUM

In the Letter "Revealing the Effects of Orientation in Composite Quasar Spectra" by J. C. Baker and R. W. Hunstead (ApJ, 452, L95 [1995]), Table 1 contained some incorrect values. A corrected version of Table 1 follows, in which relative fluxes of Hα, Mg II, C III], C IV, and Lyα have been corrected for transcript errors, as have W_λ for C IV and Lyα for $R \geq 1$.

TABLE 1

SPECTRAL MEASUREMENTS FOR MQS COMPOSITES

	$R \geq 1$			$0.1 \leq R < 1$			$R < 0.1$			CSS		
LINE	$F_{\rm rel}$ [a]	W_λ [b]	Δv [c]	$F_{\rm rel}$	W_λ	Δv	$F_{\rm rel}$	W_λ	Δv	$F_{\rm rel}$	W_λ	Δv
Hα	3.0	430	2900	6.1	660	3900	8.2	740	3200	7.2	520	2300
[O III]	0.8	71	...	0.7	91	...	1.4	250	...	4.1	340	...
Hβ	1.0	90	3500	1.0	135	5400	1.0	170	5800	1.0	83	2500
[O II]	0.1	8	...	0.03	4	...	0.07	16	...	1.7	120	...
Mg II	1.1	43	4100	1.6	75	10200	0.8	71	11200	0.7	36	7000
C III].....	1.6	34	6000	0.4	25	5500	0.4	16	6400	0.6	20	9000
C IV	3.2	50	5600	4.4	113	8900	1.5	120	8000	2.4	75	5800
Lyα.....	6.4	70	5900	...	...	...	...	...	...	2.4	79	7400
$\alpha_{\rm opt}$ [d]		0.5			0.7			1.0			1.4	
N_Q [e]		13			18			16			13	

[a] Ratio of integrated line flux relative to Hβ.
[b] Rest-frame equivalent width (Å).
[c] Velocity FWHM (km s^{-1}).
[d] Best-fit power-law spectral index, 1500–6800 Å ($f_\nu \propto \nu^{-\alpha}$).
[e] Number of quasars included in each composite.